



Investigation Nano-coating for the Corrosion Protection of Petroleum storage tanks Steel

Zainab Z. Ali*, Bahaa S. Mahdi , Ameen D. Thamer

Production and Metallurgy Engineering Dept, University of Technology-Iraq, Alsina'a Street, 10066 Baghdad, Iraq.

*Corresponding author Email: pme.19.38@grad.uotechnology.edu.iq

HIGHLIGHTS

- Using the BNi-2 alloy nano layer improves corrosion resistance.
- Applying DC sputtering as a coating method.
- Predicting generated phases for the nano-coating from EDX analysis on equilibrium phase diagrams.

ARTICLE INFO

Handling editor: Mustafa H. Al-Furaiji

Keywords:

Nano coating
AISI 1018 steel
Corrosion test
Petroleum storage tanks
BNi-2

ABSTRACT

This work studies the protection from corrosion in the inner surface of petroleum storage tanks by applying nano-coating on the AISI1018 steel type used in these tanks. BNi-2 alloy, used as coating layer, was deposited using the DC sputtering technique to obtain protection layers of nano-coating. The cyclic potential dynamic polarization technique is used to study and evaluate the resistant metal to localize corrosion, for example, pitting and crevice corrosion. The samples were evaluated in a 3.5% NaCl aqueous solution using the polarization method to determine the corrosion rate. The input parameters of deposition included ion current 16 mA, vacuum 10^{-1} mbar, time of deposition was 60 minutes, and the distance between target and substrate was 2.5 cm. The surface roughness of the uncoated specimens was (0.1466 μm), and after coating, it decreased to (0.0933 μm). The most important factor that affects the corrosion of the coated steel surface is the surface topography of steel before coating, as it is known that the sputtering process coats the facing surface to target better than the inclined surface topography. Therefore, some micro scratches non-coated well worked as nucleation for corrosion as detected in stereo microscope images for coated and uncoated surfaces. By calculating the corrosion rate from cyclic potential dynamic polarization for coated and uncoated workpieces, pitting and crevice corrosion improved approximately ten times compared to the uncoated AISI1018 steel surface.

1. Introduction

In petroleum industries, the pipeline and tank damage failure caused by corrosion represents the greatest problem in the petroleum sector, especially those buried or sub-buried within soils and water. Such an issue is the main engineering problem widely spread in many parts of the world; it represents the most well-known problem due to its important influence on projects [1,2]. According to the Iraqi environment and climate variation, many aspects affected corrosion projects involving thousands of kilometers of pipelines that transport natural gases, crude oil, and different projects beneath the surface of the earth ground tank prepared for storing [3,4]. AISI1018 steel is a major material utilized for petroleum storage tanks and transportation pipelines due to its desirable physical, chemical, and mechanical characteristics and low cost. AISI1018 steel is highly affected by corrosion where environmental conditions play an important role, particularly within the exterior corrosion of oil pipelines. Also, other factors such as the content of the petroleum products that pass through it, moisture, temperatures, pH as well as soil types influence steel corrosion rate [1,5-6]. Furthermore, corrosion affects mechanical properties, as it was found that the more acidic the soil is, the fewer the metal's tensile strength and fracture toughness will be [7]. Nano-coatings are a promising technique to control and reduce corrosion rates in the petroleum and gas industry. Nanotechnology suggested many solutions to improve the petroleum sector. It is used in the drilling process by using nano-fluid (mixing of nano-sized particles and drilling mud) to improve the petroleum drilling process and to increase crude oil production [8,9]. Nowadays, developments in surface engineering have used smart coatings and nano-coating technologies in this field. These coatings cause the most

penetration in the surface holes covered by the coating. In addition, the porosity of nano coatings is so low that the solutions that cause corrosion cannot penetrate these layers.

Furthermore, the adhesion of the gas-phase coating to the target material is very good, and coating strength is high. Because of the uniform distribution of the coating, the thin layer dispersion eliminates the potential difference and the driving force to start corrosion [10]. Nano-coating can be applied to the inner or outer surface of the petroleum industry's transportation pipelines and storage tanks, providing a smoother surface that enhances the interface's efficiency and flows on surfaces [11]. Several Nano-materials can be utilized as a thin film for petroleum industries, e.g., Al_2O_3 , Nickel, Inconel, Monel, and TiO_2 . Among all Nano-coatings, the best well-known technique used to protect thin films from corrosion is the nickel-base alloy because of its distinctive chemic, electric and optical features. BNi-2 alloy has a low absorption with high thermal and chemical stability [12]. In nanotechnology, two main techniques are used to deposit nano-materials as thin films, physical-vapor deposition (PVD) and chemical-vapor deposition (CVD). DC sputtering process is one of the physical-vapor deposition techniques. It is characterized by simplicity and efficient technique to achieve, good adherent with high mechanical specifications thin film, working in high vacuum pressures and the possibility of deposited many types of metals thin films with high quality. The target material used as the coating is bombarded with ionized gas molecules, causing atoms to be "Sputtered" off into the plasma. These vaporized atoms are then deposited when they condense as a thin film on the substrate to be coated. Many researchers revealed the effect of nanostructured thin films and the surface roughness for corrosion resistance. Gracia-Escosa et al. investigated the tribological (roughness) behavior of a TiBxCy/a-C coating prepared by Ar^+ sputtering of a combined $\text{TiC:TiB}_2(60:40)$ and graphite targets, coated on AISI 316L steel. The TiBxCy/a-C coatings film behaves as a barrier layer, improving the tribological and corrosion properties of AISI316L steel by improving the abrasion against alumina, decreasing from 0.6 to 0.1 enhancing the wear resistance [13].

A. Haniff Bharim studied the tribological aspect and mechanical properties of the nickel coating and interlayers coatings. He concluded that nickel coatings show the ability to act as lubricating. Also, he found that the surface roughness affected the corrosion behavior, tribology friction, and wear resistance. The surface roughness was reduced by applying nickel coatings, which improved tribological, mechanical properties, and corrosion resistance by improving the friction [14]. The present work aims to determine corrosion behavior in petroleum applications type AISI 1018 steel coated by BNi-2 nanoparticles as protective films using DC sputtering technique [15].

2. Experimental Work

2.1 Material Selection

The substrate material used in this study is AISI1018 carbon steel. Table 1 shows the chemical compositions of the used carbon steel, and Table 2 refers to its mechanical properties [16]. The specimens of low carbon steel were prepared with dimensions (20×20×2) mm and ground to 200 grit number to be used as substrate. BNi-2 thin foil with a 37 μm was used as a sputtering target to coat the low carbon steel specimens. Table (3) gives the chemical analysis of BNi-2 [17].

Table 1: The actual and standard chemical composition of AISI1018 [16]

Component	Fe	C	Mn	Si	Cr	Co	Nb
Standard	Bal.	0.15	0.6	0.04	0.05	---	---
AISI1018 wt%		-0.2	-0.9	Max	Max		
Actual wt%	Bal.	0.18	0.75	0.22	0.09	0.03	0.02.

Table 2: The mechanical properties of AISI 1018 [16]

Property	Yield Strength (MPa)	Ultimate Strength (MPa)	Elongation, %	Modulus of Elasticity (GPa)
Value	370	440	15	205

Table 3: The chemical composition of the target (BNi-2) [17]

Product name	AWS A5.8	Nickel	Chromium	Iron	Silicon	Boron
Ni-83	BNi-2	Bal	7	3	4.5	3

2.2 Thin-film Preparation Using DC Sputtering

The DC sputtering unit included a vacuum system consisting of a rotary vacuum pump and a vacuum chamber constructed from high-temperature Pyrex glass. The Ion current of the process was 16mA, the distance kept constant between target and substrate was 2.5 cm, and the pressure vacuum was 10^{-1} mbar. Figure 1 shows the photograph of the work unit with the sputtering system. First, the BNi-2 disc was adjusted in the sputter chamber. Then, the chamber was evacuated using a rotary pump to arrive at the required operating pressure. The bombardment of the target with gas ions will erode this target material. After that, films grow on the substrate of the AISI1018 material. During the coating process, the pressure was kept constant at 10^{-1} mbar.

2.3 Corrosion Study

The corrosion solution comparable to seawater was prepared through a 3.5 wt% NaCl solution by adding 35 grams of NaCl to a liter of distilled water at room temperature. The cyclic potential dynamic polarization was carried out using the potential state as shown in Figure 2.

3. Results and Discussion

3.1 Topography and Microstructure

The surface roughness value is measured using a roughness device model (MAHR GMBH made in Germany) in the university of technology – Production and Metallurgy department.

The surface roughness of the specimens before the coating was (0.1466 μm) and was (0.0933 μm) after coating. The surface topography was inspected using the stereo microscope (8549,33 made in Italy) in the Production and Metallurgy Department / University of Technology.

The topography of the coated specimens, as shown in Figure 3, shows the image of the completely coated with BNi-2, except for some small points and scratches representing less than 1% of the total coated area.

The cause of these non-coated areas is the nature of the sputtering process, where the direction of target sputtered atoms was facing the substrate surface. Because of this, any deep spots will suffer from low-sputtered-atom concentrations and cause poor coating layers. Likewise, the grinding grooves suffer from the same phenomenon.

So, to obtain a completely coated substrate surface, the surface must be highly polished, but polishing leads to the low adhesion of the coating layer due to the small real surface area of the prepared substrate [18].

The samples were prepared with a certain degree of roughness for mechanical interlocking between the substrate and the coating and to obtain a higher adhesion. Still, this roughness (tops and bottoms) on the substrate's surface can be considered a nuclear for pit formation, which becomes an anodic area when exposed to the corrosion solution. This leads to a concentration of chloride ions, but the vast area that acts as a thin film becomes cathodic, thus leading to severe galvanic corrosion. On the other hand, the base metal has been exposed to general uniform corrosion because the roughness increases the rate of corrosion [19,20].

Figure 4 represents the surface of the coated specimens after the corrosion test with some corroded coat layers. After investigating this area, it can be concluded that the small uncoated regions by the sputtering process work as a nucleation source of corrosion that spreads continuously with time and removes the neighboring coat layer. Furthermore, based on the topographic results, it can be noted that substrate roughness plays an important role in affected corrosion.

Figure 5 represents the uncoated micrograph image of steel specimens, and Figure 6 shows intensive corrosion for the uncoated specimen after the corrosion test, where the entire surface suffered from material loss because, as it is known, low carbon steel is very weak against corrosion. However, comparing corrosion tests for the coated and non-coated substrate surfaces, it can be found that, even with a thickness of some nanometers, the coating layer can work as an excellent protective layer against corrosion in coating conditions uniformly for all the uncoated surfaces, even for small regions that expand corrosion to the surrounded areas.

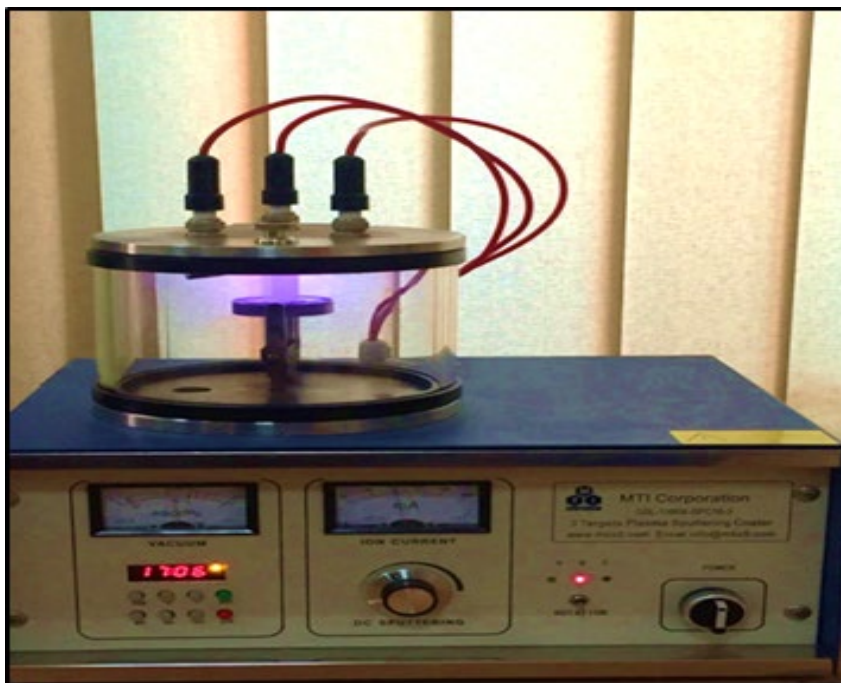


Figure 1: The thin film preparation unit uses DC sputtering technique



Figure 2: Figure 2: The cyclic potential dynamic polarization test device

3.2 Thickness Measurements

Measuring nano-coating thickness needs high SEM magnification and special specimen preparations. So, sectioning and traditional sample preparation cannot be done here due to the destruction of the nanolayer during sample preparation. However, scratching the coated surface using a sharp blade, magnifying the scratch residue beside the groove, and finding some normal pieces to angle of view help to measure its thickness, giving good accuracy.

Figure 7 represents SEM morphology for scratched BNi-2 alloy deposited on glass with the same parameters and coating batch done on AISI 1018 steel. Glass is used because it is hard to scratch compared to steel and gives good surface identification in SEM after coating the sample by sputtering with a nano gold layer of not more than 5 nm. The average BNi-2 coat thickness is around 120 nm. A general surface morphology shows a dense and excellent homogeneous microstructure and large area uniformity. In addition, the coating layer, as observed under SEM, was found to be crack free. In this case, the coating layer was featureless due to the smooth surface nature of glass and the mode of the sputtering process, that is, the deposition of coat atoms in a parallel and regular form on the substrate.

Examine the coated steel surface by energy dispersive X-ray analysis (EDX). The EDX microprobe gives the chemical composition of the interphases between the BNi-2 coating and 1018 AISI steel. The EDX analysis of the interphase shown in Figure 8 suggests that some diffusion has occurred between Fe and the BNi-2 coating. It can be observed that there is a reduction in the concentrations of Fe and Ni in the interphase regions (52.35 and 24.71 wt.% for Fe and Ni, respectively), which is lower than that of the substrate Fe concentration (52.34 wt%) and the resulting phases are (α Fe+ γ Ni) according to Figure 9.

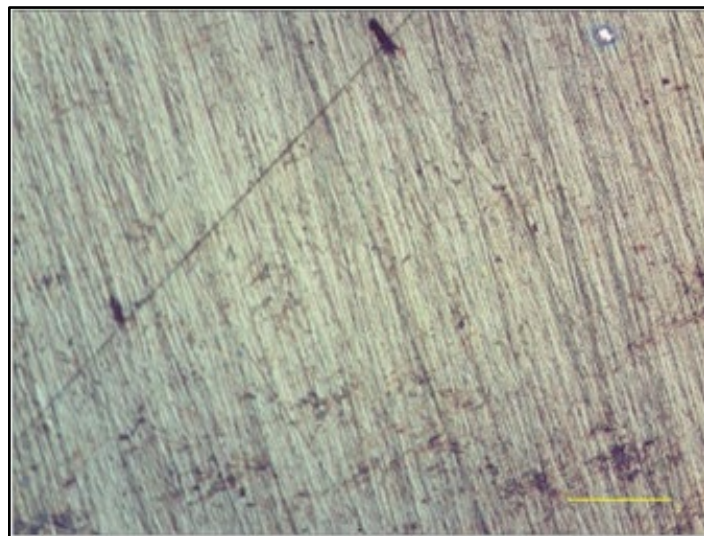


Figure 3: Coated specimen before corrosion (60X).

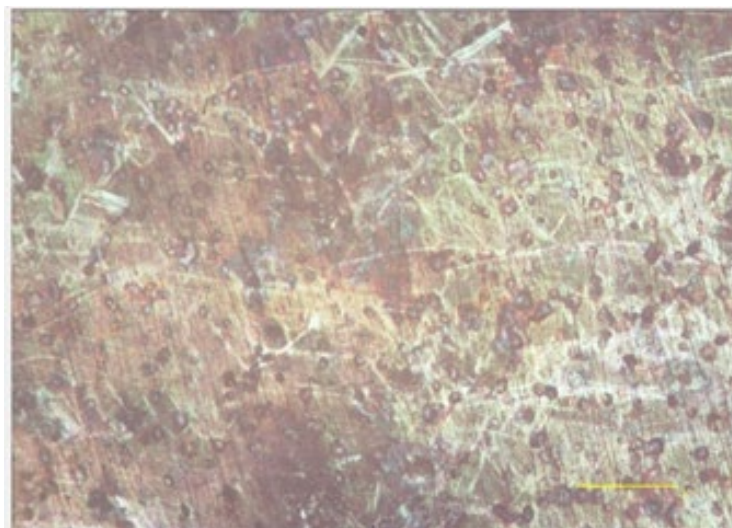


Figure 4: Coated specimen after corrosion (60X).

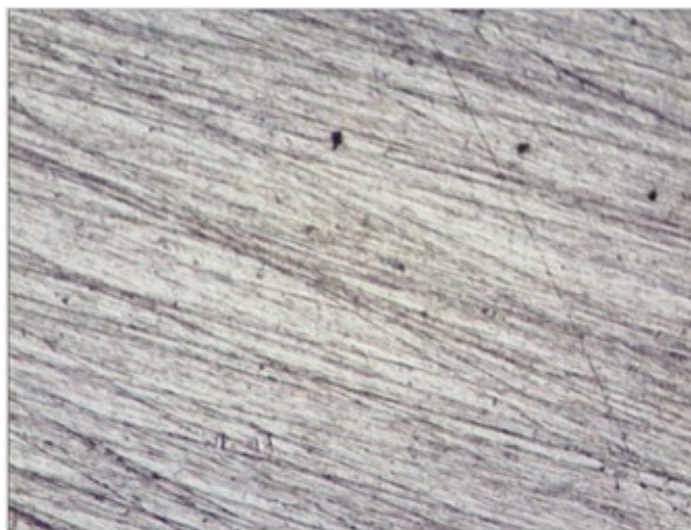


Figure 5: Uncoated specimen before corrosion (60X).

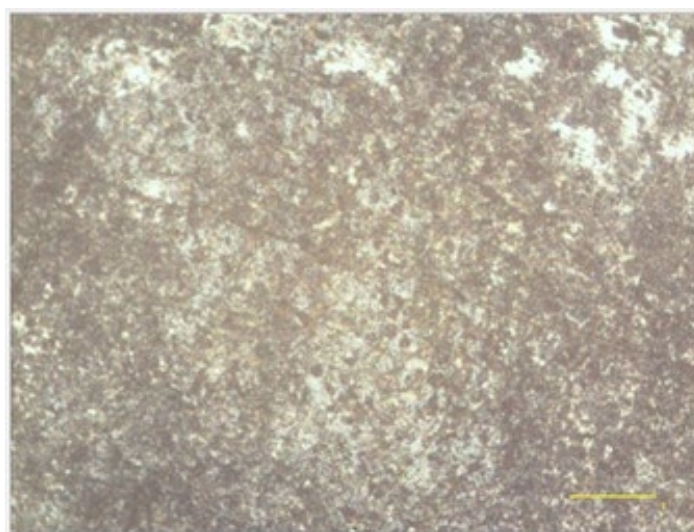


Figure 6: Uncoated specimen after corrosion (60X).

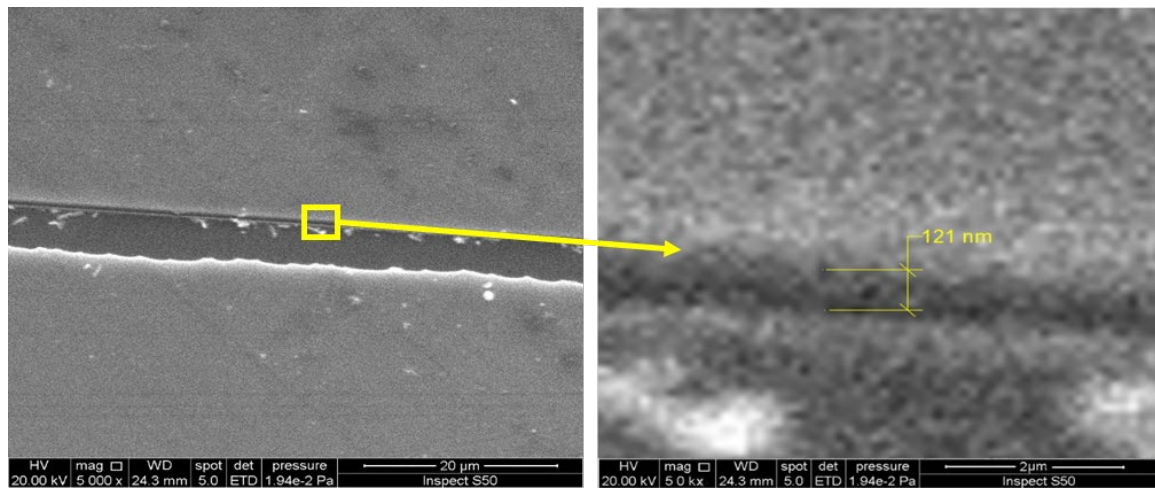


Figure 7: SEM images of the scratched coat of NBi-2 deposited on glass (left 5kx, right 50kx).

3.3 The Cyclic Potential Dynamic Polarization Technique

Figure 10 shows the cyclic potential dynamic polarization (CPDP) for NBi-2 coated and uncoated workpieces obtained in a 3.5% NaCl aqueous solution.

Once passing through the zone of active corrosion, the present density drops to a serious potential, known as the “primary passivation potential”. Such a decrease might be attributed to the creation of the non-active layer upon the metal surface as oxides, which is a non-electrically conductive layer [22]. The current density in the non-active zone is called the non-active current density. Increasing the potential in the non-active zone enables one to detect a quick rise in the anodic current. The rise can be attributed to either oxygen’s evolution because of the water’s decay or the breaking of the non-active film and localized corrosion [23]. The zone can be named “transpassive zone”. The reason for such an increase in current density is water decomposition and oxygen gas evolution [23]. The increase caused by the anodic current density at the potential under the oxygen evolution potential represents the beginning of pitting as well as the occurrence of localized corrosion (E_{pit}) [22,23]. To make a comparison between coated and non-coated specimens, the corrosion rate can be calculated according to the equation below [22] which represent the corrosion rate of one milli inch per year:

$$\text{Corrosion rate (mpy)} = 0.129 \times \dot{i}_{corr} \times Ew/d \quad (1)$$

Where Ew is equivalent weight, which is 55.84 and 58.69 for steel and nickel respectively; d is a density, which is 7.86 and 8.9 g/cm³ for steel and nickel individually, and \dot{i}_{corr} is the corrosion current density that obtained from curves, 0.0026 and 0.023 mA for coated and uncoated respectively, the area exhibition directly to corrosion during test was constant for tow specimens is 1.2271cm².

By applying the equation (1) for these conditions \dot{i}_{corr} for coated specimen was 0.002118mA/cm² (2.118μA/cm²) and the corrosion rate is (1.802) mpy while the I_{corr} for uncoated specimen is 0.01874mA/cm² (18.7433μA/cm²) and the corrosion rate was (17.17) mpy which is approximately about 9.5 times greater than the coated specimen

It can be noticed that the corrosion potential for the coated sample is approximately equal to -410 mV, which is nobler than that of the uncoated sample, which is -500mV. The uncoated workpiece causes a high corrosion current compared to the coated one. The improvement for the BNi-2 coated workpiece is about 10 times greater than that for the uncoated workpiece. This might be ascribed to fewer coating flaws, such as holes and crashes.

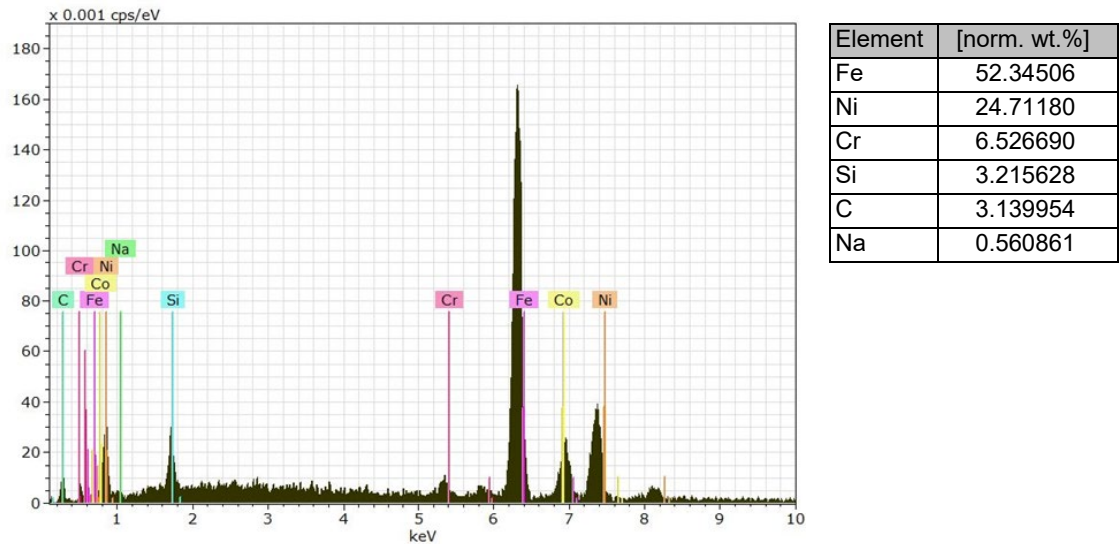


Figure 8: EDX test of the interphases between BNi-2 coating and steel

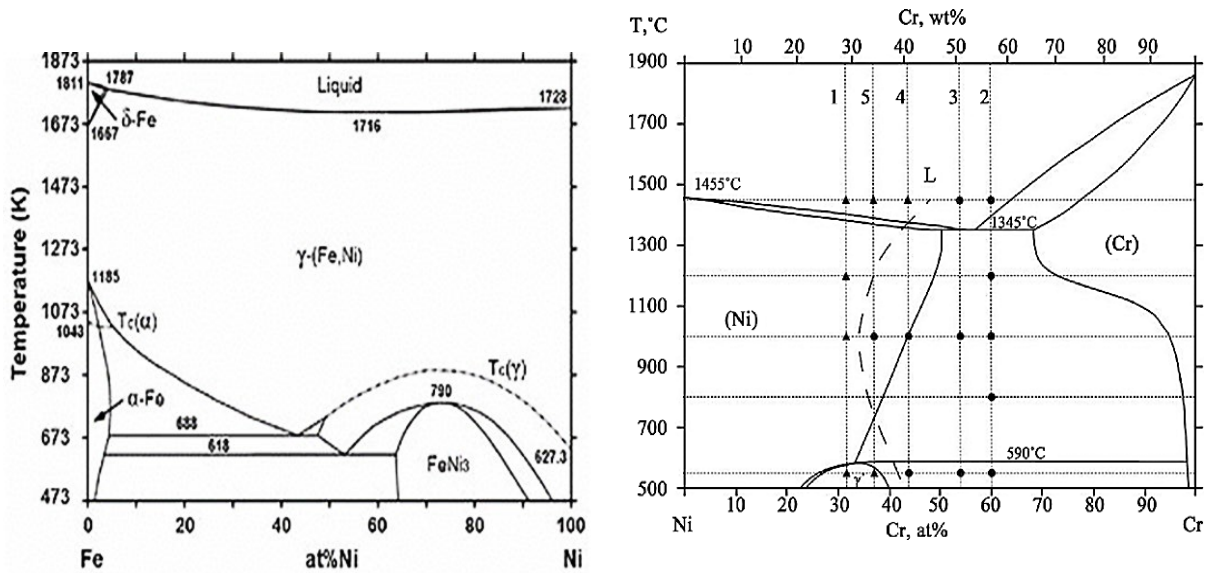


Figure 9: Binary thermal equilibrium diagrams for (Fe-Ni) and (Ni-Cr) [21]

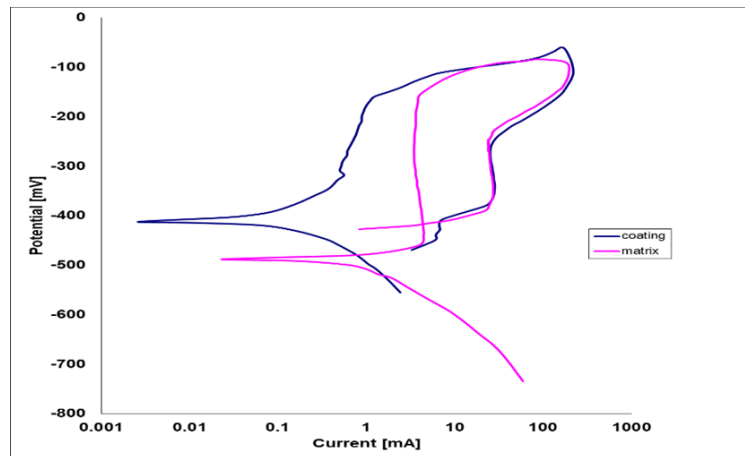


Figure 10: Cyclic potential dynamic polarization for BNi-2 coated and uncoated workpieces work pieces

4. Conclusion

1. The role of seawater (NaCl) ions and the effect of coating with BNi-2 thin film were studied for the corrosion rate of petroleum storage tank steel. As a result, the corrosion rate decreased from 17.17 mpy to 1.802 mpy by applying BNi-2 nano-coating on 1018 AISI steel.
2. The increase in corrosion resistance is attributed to forming a barrier to prevent the metallic surface from being contacted with chloride ions, considered the most aggressive corrosive species.
3. The nano-thickness of the BNi-2 thin film can improve corrosion resistance by order of 10 times more than uncoated 1018 AISI steel.
4. From the morphology observations after the corrosion test by a stereo microscope, uncoated AISI 1018 steel has general corrosion, but the coated specimen has localized pitting corrosion. That is due to small uncoated regions by spattering that act as nucleation sources of corrosion that spread continuously with time and remove the neighboring coat layer. Based on the topographic results, it can be noted that substrate roughness plays an important role in affecting corrosion.
5. Applying the coating layer using the DC sputtering technique decreases the surface roughness by about 0.0533 μm of the coated substrate.
6. Surface roughness is useful for the adhesion of the thin layer to a substrate, but it prevents some local areas from the coating, which acts as a nucleation site for pitting and crevice corrosion.

Acknowledgment

The contribution in the current work was equally made by all authors.

Funding

No grant is provided to the present work and given by any funding organization within the public, commercial, or not-for-profit sector.

The Statement of Data Availability

Upon any demand made by the corresponding author, the data which supports the conclusions of the current work can be made available.

Conflict of Interest

There is no conflict of interest in the current work.

References

- [1] M. M. Mirza, E. Rasu, A. Desilva, Influence of Nano Additives on Protective Coatings for Oil Pipe Lines of Oman, *Int. J. Chem. Eng.*, 7 (2016) 221-225. <https://doi.org/10.18178/ijcea.2016.7.4.577>
- [2] E. Noveiri, S. Torf, Nano Coating Application for Corrosion Reduction in Oil and Gas Transmission Pipe: A Case Study in South of Iran, *Int. Conf. Adv. Mater.Eng.*, 15, 2011.
- [3] Q. J. Sulaiman, A. Al – Taie , D.M.Hassa, Evaluation of Sodium Chloride and Acidity Effect on Corrosion of Buried Carbon Steel Pipeline in Iraqi Soil, *Iraqi J. Chem. Pet. Eng.*, 15 (2014) 1-8. <https://doi.org/10.31699/IJCPE>
- [4] A. D. Usmana, L. N. Okoro, Mild Steel Corrosion in Different Oil Type, *Int. J. Sci. Res. Innov. Technol.*, 2 (2015) 9-13.
- [5] C.Matteo, P.Candido, R. Vera, V. Francesca, Current and Future Nanotech Applications in the Oil Industry, *Am. J. Appl. Sci.*, 9 (2012) 784-793. <https://doi.org/10.3844/ajassp.2012.784.793>
- [6] G.Balakrishnan, Effect of substrate temperature on microstructure and properties of nanocrystalline titania thin films prepared by pulsed laser deposition, *nanosystems: physics, chemistry, mathematics*, 7 (2016) 621–623. <https://doi.org/10.17586/2220-8054-2016-7-4-621-623>
- [7] Y. Hou, D. Lei, S. Li, W. Yang, C-Q. Li, Experimental Investigation on Corrosion Effect on Mechanical Properties of Buried Metal Pipes, *Int. J. Corros.*, 2016 (2016)13. <https://doi.org/10.1155/2016/5808372>
- [8] S. Murugesan, Pulsed laser deposition of anatase and rutile TiO₂ thin films, *Metallurgy and Materials Group, IGCAR*. 201 (2007) 7713– 7719. <https://doi.org/10.1016/j.surfcoat.2007.03.004>
- [9] Y. Zhao, C. Chen, Influence of the technical parameters on bioactive films deposited by pulsed laser, *Surf. Rev. Lett.*, 14 (2007) 283-191. <https://doi.org/10.1142/S0218625X07009372>
- [10] N. M. mohammadi, Molood Barmala, Investigating the Effect of Nano Technology on Increasing Utilization in Oil Tanks and Wells in Upstream Industries, *Int.J. New Chem.*, 6 (2019)289-298. <https://doi.org/10.22034/IJNC.2019.34458>
- [11] R. Singh, *Corrosion Control for Offshore Structures: Cathodic Protection and High Efficiency Coating*, Gulf Professional Publishing: Waltham, MA, USA, 2015.<https://doi.org/10.1016/C2012-0-01231-8>

- [12] A. Shanaghi, A. S.Rouhaghdam, M. Aliofkhazraei, Study of TiO₂ nanoparticle coatings by the SOL-GEL methods for corrosion protection, *Mater. Sci.*, 44 (2008) 233-247. <https://doi.org/10.1007/s11003-008-9070-6>
- [13] B. Grančič, M. Mikula, T. Roch, Effect of Si Addition on Mechanical Properties and High Temperature Oxidation Resistance of Ti-B-Si Hard Coatings, *Surf. Coat. Technol.*, 240 (2014) 48-54. <https://doi.org/10.1016/j.surfcoat.2013.12.011>
- [14] A. H.Bharim, Tribology of Electroless Nickel and Interlayer Coatings, A Review, *IOP Conf. Ser.: Mater. Sci. Eng.*, 1068,2021,012011. <https://doi.org/10.1088/1757-899X/1068/1/012011>
- [15] M. J. Kadhim, K. A. Sukkar, A. S. Abbas, N. H. Obaeed, Investigation Nano coating for Corrosion Protection of Petroleum Pipeline Steel Type A106 Grade B, Theoretical and Practical Study in Iraqi Petroleum Sector, *Eng. Technol. J.*, 35 (2017) 1042- 1051. <https://doi.org/10.30684/etj.35.10A.11>
- [16] Autoren Wegst, C. and Wegst , M. Key to steel,part 1 , 2004.
- [17] ASM Metals Handbook, Properties and Selection: Nonferrous Alloys and Special-Purpose Materials, ASM Handbook, 1990. <https://doi.org/10.31399/asm.hb.v02.9781627081627>
- [18] J.-L. Trausch and F.H. Wittmann, Surface roughness and adhesion, Conference: Durable Concrete Structures, Int. Workshop on Properties and DesignAt: Weimar, Germany,1998.
- [19] H. M. Abdulmajeed, Hiba A., Abdullah, Slafa I. Ibrahim, Ghaith Z. Alsandoq , Investigation of Corrosion Protection for Steel by Eco-Friendly Coating, *Eng. Technol. J.*, 37 (2019) 52-59. <http://dx.doi.org/10.30684/etj.37.2A.3>
- [20] U. Sajjad, A. Abbas, Ali. Sadeghianjahromi, N. Abbas, Jane-SunnLiaw, Chi-Chuan Wang, Enhancing corrosion resistance of Al 5050 alloy based on surface roughness and its fabrication methods, an experimental investigation, *J. Mater. Res. Technol.*,11 (2021) 1859-1867.<https://doi.org/10.1016/j.jmrt.2021.01.096>
- [21] Okamoto,H. Alloy Phase Diagrams, ASM Metals Handbook, 2016.<https://doi.org/10.31399/asm.hb.v03.9781627081634>
- [22] Z. Ahmad, CHAPTER 7 - COATINGS ,Principle of corrosion engineering and corrosion control , 2006. <https://doi.org/10.1016/B978-075065924-6/50008-8>
- [23] Stephen D. Cramer; Bernard S. Covino, Jr. Corrosion: Fundamentals, Testing, and Protection, ASM Handbook,2003 <https://doi.org/10.31399/asm.hb.v13a.9781627081825>